Cholesterol Binding to Cytochrome P450 7A1, a Key Enzyme in Bile Acid Biosynthesis†

Natalia Mast,‡ Sandra E. Graham,§ Ulla Andersson,|| Ingemar Bjorkhem,|| Courtney Hill,‡ Julian Peterson,§ and Irina A. Pikuleva*,‡

Department of Pharmacology and Toxicology, University of Texas Medical Branch, Galveston, Texas 77555-1031, Department of Biochemistry, University of Texas Southwestern Medical Center, 5323 Harry Hines Boulevard, Dallas, Texas 75390-9038, and Department of Clinical Chemistry, Karolinska Institute, Huddinge Hospital, S-141 88, Huddinge, Sweden

Received November 19, 2004; Revised Manuscript Received December 21, 2004

ABSTRACT: The conversion of cholesterol to 7α-hydroxycholesterol catalyzed by cytochrome P450 7A1 (CYP7A1) initiates the major pathway for cholesterol elimination in mammals. In the present work we focused on identification of determinants of the CYP7A1 substrate specificity inside the active site using a homology model with a novel P450-fold, site-directed mutagenesis, and substrate-binding and kinetic studies. Forty-one mutants, encompassing twenty-six amino acid residues, were generated and characterized, and of these, seven residues appear to determine cholesterol binding in the active site. In addition, four cholesterol derivatives were used as active site probes in the wild type and the seven mutant enzymes, and the spectral binding constants and products were analyzed. It was concluded that Asn288 in the I helix plays a key role in the P450−cholesterol contacts by hydrogen bonding to the steroid 3*β*-hydroxyl, while Val280 and Ala284 are beside and the Trp283 is above the steroid nucleus orienting the cholesterol molecule. Leu360 and Ala358 between the K helix and the *β*1−4 strand and Leu485 in the *β*4 sheet−turn appear to define the size of the active site over the heme pyrrole ring A, thus limiting the orientation and size of the substrate at the steroid A ring. Additionally, the A358V mutant was found to form two new products, one being 7*β*-hydroxycholesterol. Our data indicate that a tight fit of cholesterol in the enzyme active site is in part responsible for the high efficiency of cholesterol turnover by CYP7A1.

In mammals, cholesterol elimination is achieved mainly through its conversion to bile acids (*1*). While several metabolic routes lead to the formation of bile acids, the route which begins with the hydroxylation of the cholesterol ring system dominates under normal physiological conditions (*2*). This route is called the classical or neutral bile acid biosynthetic pathway. It occurs in the liver and is initiated in the endoplasmic reticulum by cytochrome P450 7A1 (CYP7A1),[1] which catalyzes the conversion of cholesterol to 7α-hydroxycholesterol (*3*). The importance of this enzymatic reaction is highlighted by the fact that cholesterol 7α-hydroxylase deficiency in humans results in high levels of total serum and LDL cholesterol, substantial accumulation of cholesterol in the liver, and a markedly decreased rate of bile acid excretion as assessed by the examination of individuals with a homozygous mutation in the *CYP7A1* gene that abolished the enzyme function (*4*). Studies of CYP7A1 substrate specificity indicate that the steroid has to have a free hydroxyl group at C3 and a *trans* or quasi-*trans* A/B ring configuration (*3*). Requirements for the substrate side chain are not as stringent as for the ring system as shown by the ability of CYP7A1 to metabolize such cholesterol derivatives as 20*S*-, 24*S*-, 25-, and 27-hydroxycholesterols in the reconstituted system in vitro and in COS cells (*5*, *6*). Surprisingly, little is known about the residues in the CYP7A1 active site that are involved in the interaction with cholesterol. Several years ago this laboratory initiated systematic structure/function studies of CYP7A1 which capitalize on the knowledge derived from the analysis of crystal structures of different P450s and of models based on these structures (*7*−*12*). Despite ≤20% sequence identity, all structurally characterized P450s have a similar overall fold with the active site formed by the same secondary structural elements. In some of the structurally determined P450s, the active site is isolated from the protein surface, but in most there is one or more clear channels between the buried active site and the protein exterior. Crystallographic studies of P450 102A1, a soluble bacterial P450, indicate that a hydrophobic patch of amino acids at the mouth of the substrate access channel located near *β*-strands 1−1/1−2 and the F−G loop could participate in initial substrate recognition (*13*). On the other hand, in eukaryotic membrane-associated

† These studies were supported in part by U.S. Public Health Service Grants GM62882 (to I.A.P.) and GM43479 (to J.P.), a grant from the Swedish Medical Research Council (to I.B.), NIEHS Center Grant ES06676, and the Howard Hughes Medical Institute 1999 Biomedical Research Support Program for Medical Schools, Grant 53000266.

* To whom correspondence should be addressed. Tel: (409) 772-9657. Fax: (409) 772-9642. E-mail: irpikule@utmb.edu.

‡ University of Texas Medical Branch.

§ University of Texas Southwestern Medical Center.

|| Karolinska Institute.

[1] Abbreviations: CYP7A1, cytochrome P450 7A1; *E. coli*, *Escherichia coli*; GC-MS, gas chromatography−mass spectrometry; HPCD, 2-hydroxypropyl-*β*-cyclodextrin; HPLC, high-pressure liquid chromatography; KP_i, potassium phosphate buffer; TMSi, trimethylsilyl.

10.1021/bi047566a CCC: $30.25
Published on Web 02/10/2005

P450s such as CYP2C5, their hydrophobic substrates are most likely recruited directly from the lipid bilayer (*8*, *12*). It also was suggested that residues lining the interior of the channel can control the orientation of the substrate as it enters the enzyme active site and provide an additional mechanism for the strict regioselectivity of hydroxylation reactions in addition to the residues inside the active site (*8*, *14*). Thus, substrate specificity in P450s that regioselectively hydroxylate a limited number of structurally similar substrates could be governed by three groups of residues which are located on the surface of the molecule, inside the substrate access channel and inside the active site. Previously, we investigated the role of the putative F−G loop in CYP7A1, a surface region of the P450 structure, which was shown to be important for substrate access/interaction in a number of structurally characterized P450s (*15*−*19*) and predicted to be associated with the membrane in eukaryotic P450s (*8*, *12*). Mutations within this region affected interaction of recombinant enzyme with the *Escherichia coli* membrane, decreased k_{cat} and significantly increased K_m, but not the K_d for cholesterol (*20*). On the basis of these data, we proposed that the putative F−G loop is one of the membrane-interacting areas in CYP7A1, whereby cholesterol enters the enzyme from the membrane, and residues at the membrane−protein interface participate in initial cholesterol recognition (*20*). Herein, we have used mutagenesis studies, molecular modeling, and cholesterol analogues to gain further insight into the mechanism for CYP7A1 substrate specificity by identifying a set of residues in the enzyme active site that we believe are involved in the interaction with cholesterol.

EXPERIMENTAL PROCEDURES

CYP7A1 Sequence Alignment, Modeling, and Cholesterol Docking. The modeling of CYP7A1 was done using an approach in which three determined P450 structures were used as templates. The templates used for the first generated structure were substrate-free P450BMP which is the heme domain of P450 102A1 (CYP102A1; PDB code 2HPD), substrate-free CYP2C5 (PDB code 1DT67), and CYP51 (PDB code 1EA1). The second generation model shown in this paper was generated using substrate-bound P450 102A1 (1JPZ), substrate-bound CYP2C5 (1N6B), and CYP51 (1EA1). A structural alignment of the three proteins was done using the Homology suite of InsightII (Accelrys, Inc.). The sequence of CYP7A1 was then aligned to the template sequences initially using the ClustalW program and, then, further refining this alignment manually to ensure that the known conserved sequences and patterns were aligned and that the amphipathicity of helices was in register. Using these alignments, the Modeler program of the InsightII suite was employed to generate two or three models with three sets of loops each. The model selected for further study was the one with the fewest buried unpaired charges. This model was then energy minimized using the Discover package of the InsightII suite until the change in energy with respect to the change in the coordinates was less than 0.01. The substrate was then introduced into the substrate-binding pocket, docked manually, and then optimized using either molecular dynamics or Affinity (Accelrys, Inc.) or HEX (www.biochem.abdn.ac.uk/hex/) to optimize the orientation.

Site-Directed Mutagenesis. A truncated form of a human CYP7A1 in which the N-terminal membrane anchor was removed by genetic engineering (*20*) was used in the present study. Site-directed mutagenesis was carried out using an in vitro QuikChange site-directed mutagenesis kit (Stratagene) according to the instructions. The mutagenic oligonucleotides are shown in Table 1 of Supporting Information. The correct generation of desired mutations and the absence of undesired mutations were confirmed by DNA sequencing of the entire CYP7A1 coding region. The expression of CYP7A1 and the various mutant forms in *E. coli* and partial purification were as described (*20*).

Substrate-Binding Assays. Several approaches were used to characterize substrate binding to CYP7A1. In all of these approaches the assay buffer was always 50 mM potassium phosphate buffer (KP_i), pH 7.4, containing 20% glycerol, 0.05% Tween 20, and 1 mM EDTA, and substrates were added from a stock solution (1−10 mM) in 2-hydroxypropyl-β-cyclodextrin (HPCD). Tween 20 was included because previously we investigated the effect of 0.01%−0.4% Tween 20 on the enzyme activity and found that at 0.01%−0.05% concentrations this detergent stimulates the activity whereas at higher concentrations it starts inhibiting the activity. The maximal stimulation of the activity (more than 4-fold compared with the detergent-free buffer) was observed at 0.05% Tween 20. At this concentration, however, Tween 20 increases the K_d of cholesterol for CYP7A1 about 90-fold, from 0.05 μM in detergent-free buffer to 4.4 μM in the presence of 0.05% Tween 2. To be able to compare substrate-binding and kinetic properties of CYP7A1 wild type and mutants, the K_d and K_m values must be measured in the same assay buffers, so we decided to include 0.05% Tween 20 in the buffer for substrate binding. Initially, all probe substrates were assessed for the ability to induce a 420−390 nm shift in the spectrum of P450 (type I spectral response). If a substrate-induced spectral shift was observed, titrations with steroids were carried out in 1 mL of the assay buffer at 0.1−0.5 μM P450 concentrations. The total volume of the added steroid was no more than 10 μL. GraphPad Prism software (GraphPad, San Diego, CA) was used to calculate apparent binding constants (K_d) by fitting spectral data into one of the following equations: $\Delta A = (\Delta A_{max}[S])/(K_d + [S])$ or $\Delta A = 0.5\Delta A_{max}(K_d + [E] + [S] - ((K_d + [E] + [S])^2 - 4[E][S])^{1/2})$, where ΔA is the spectral response at different substrate concentrations [S], ΔA_{max} is the maximal amplitude of the spectral response, and [E] is the enzyme concentration. The former equation was applied when K_d was higher than the enzyme concentration and the latter when K_d was similar to or less than the enzyme concentration assuming 1:1 stoichiometry. After each experiment, the P450 content was quantified by the CO difference spectrum of the reduced form of the enzyme (*21*) to confirm that there was no denaturation during titration.

Some of the cholesterol analogues did not induce a spectral shift, and they were tested for the ability to displace cholesterol from the P450 active site (displacement assay). This approach was utilized previously to determine affinities of several compounds that do not yield difference spectra to CYP2D6 (*22*). Two P450 samples were balanced against each other in a spectrophotometer, and then cholesterol was added to the sample cuvette to 5 μM, a value near the K_d of cholesterol for CYP7A1 (4.3 μM, determined experimentally from the spectral binding assay) to induce a type I spectral response. Then varying amounts of the probe substrate (1−

50 μM) from 1 or 10 mM stock were added to the sample cuvette, and spectral changes, $\Delta A_{390-420}$, were plotted vs the concentration of the probe substrate and the concentration of the added HPCD. Then, in a separate experiment, P450 in the presence of 5 μM cholesterol was titrated with a 45% solution of HPCD that was used to dissolve the probe substrate to account for the effect of this vehicle on cholesterol binding to P450, and the $\Delta A_{390-420}$ plots vs HPCD concentration were subtracted from those obtained during titration with the probe substrate. Analysis of the corrected spectra indicates that none of the probe substrates tested (5-cholestene, 5-cholesten-3β-ol methyl ether, and cholesterol sulfate) caused attenuation of the cholesterol-induced spectral response, suggesting that these compounds do not displace cholesterol from the CYP7A1 active site, likely because they do not bind to the active site. To confirm that, the K_d and ΔA_{max} of cholesterol for CYP7A1 in the presence of 20 μM probe substrate were determined (inhibition assay). Neither K_d nor ΔA_{max} was affected by the probe substrates, providing further evidence that they do not bind to the enzyme active site. Specially for the present study we also developed a filter binding assay to characterize mutants that did not show spectral response upon addition of cholesterol or exhibited reverse type I spectral response (a shift from 390 to 420 nm) or had a significantly reduced ΔA_{max} in a spectral binding assay. A detailed description of this assay will be published separately. This assay was conducted in small glass test tubes, each containing the assay buffer, 1 μM P450, 1 nM [^{3}H]-cholesterol (250000 cpm), and a range of cold cholesterol (0−50 μM) in a total volume of 50 μL. Reagents were mixed and incubated on ice for 30 min, and then the content of each tube was filtered onto a premoistened ICE 450 polysulfone membrane (pore size 0.45 μm, diameter 47 mm) from Pall Life Science (Ann Arbor, MI). Filters were washed with 1 mL of the assay buffer, dried for 3 h at 37 °C, placed in 5 mL of scintillation liquid, and counted. The data were corrected for the nonspecific binding (~6%) of the [^{3}H]-cholesterol to the filter in the absence of P450 and cold cholesterol. Then radioactivity of the filters at various concentrations of cold cholesterol was subtracted from the radioactivity of the filter when no cold cholesterol but only P450 was present in the assay buffer, and the resulting data were plotted vs the concentration of cold cholesterol and fit as described for the spectral binding assay. About 85% of radioactive cholesterol was displaced in the wild-type CYP7A1 by cold cholesterol at saturating cholesterol concentrations, indicating that ~15% of this substrate was bound nonspecifically to the P450. The amount of P450, 50 pmol, used in this assay was selected on the basis of our data on the maximal capacity of the filter to bind the enzyme: no CYP7A1 was detected in the flow-through fraction when 25, 50, and 75 pmol were used, whereas ~10% of the enzyme went through the filter when 100 pmol was used. Radioactive and cold cholesterol were added from stock solutions in 45% HPCD, and the total volume of 45% HPCD was adjusted to 5 μL. In a separate experiment we established that up to 10 μL of 45% HPCD could be used in the assay without effect on cholesterol binding to P450. Independent of whether cholesterol was added from 1 mM stock in 4.5% or in 45% HPCD, kinetic constants were essentially the same.

HPCD was used in the present study to prepare stock solutions of steroids because when dissolved in organic solvent (ethanol, acetone, dimethylformamide, or acetonitrile), cholesterol induced a very small spectral response in CYP7A1 at 1−20 μM concentrations, and this response was distorted by the turbidity because of cholesterol precipitation upon dilution into aqueous solution. A poor spectral response precluded utilization of a spectral binding assay; therefore, we tested HPCD. HPCD solubilizes hydrophobic compounds by forming an inclusion complex in which the solubilized lipophile is partially inserted in the hydrophobic cavity of HPCD (*23*). The advantage of cyclodextrin-solubilized compounds is that they do not precipitate upon dilution in aqueous medium, and in the case of moderately to weakly to bound lipophiles (binding constants of 100 μM or higher), their release from the cyclodextrin inclusion complexes is essentially instantaneous and quantitative (*24*). The average lifetime of a lipophile in the cyclodextrin cavity was found to be in the milli- to microsecond time range or shorter dependent upon the compound with simple dilution being the major driving force for dissociation of weakly to moderately bound complexes (*24*). HPCD appeared to be the only vehicle in which cholesterol induced a substantial type I spectral response in CYP7A1 with no turbidity and with the $\Delta A_{390-420}$ increased up to 9 μM cholesterol concentration and then stayed unchanged up to 100 μM concentration. The K_d of cholesterol for HPCD in the assay buffer was determined. The K_d measurement was based on the approach utilized by others (*25*), in which turbidity of a solution containing a suspension of a hydrophobic compound is decreased in the presence of increasing concentrations of HPCD. To ensure that measurements are taken at the solubility equilibrium, a 0.5 mM suspension of cholesterol in the assay buffer was divided into 20 aliquots to which different amounts of HPCD from 45% stock solution were added. Aliquots were left at room temperature and under constant stirring and their optical densities (due to turbidity) measured at 450 nm on the 16th and 40th h following the addition of HPCD with essentially no difference between the values at two time points. The range of HPCD concentrations used was 0%−7.5% (0−63 mM), the optical density of the aliquot in the absence of HPCD was 0.18, and that of six aliquots with 1.2%−7.5% (10−63 mM) HPCD was zero, indicating that cholesterol was completely dissolved. The optical density of an aliquot at a given concentration of HPCD was then subtracted from the optical density of the cholesterol suspension in the absence of HPCD, and the data obtained were plotted vs HPCD concentration. The K_d was calculated with GraphPrism from software using the following equation: $A = 0.5A_{max}(K_d + [C] + [HPCD] - ((K_d + [C] + [HPCD])^2 - 4[C][HPCD])^{1/2})$, where A is the optical density at different HPCD concentrations [HPCD], A_{max} is the maximal optical density, and [C] is the cholesterol concentration. Because oligomers of glucose in HPCD have a different degree of substitution, usually percent solutions of HPCD are prepared. However, to compare the K_d value of cholesterol for HPCD with that for P450, the same units must be used; therefore, we converted percent concentrations of HPCD into micromolar concentrations knowing that mixing 45 g of HPCD with 55 mL of water produces 82 mL of solution, and the average molecular weight of HPCD from Sigma-Aldrich (catalog number CO926) is 1450. The K_d value of cholesterol for HPCD in 50 mM KP_i, pH 7.4, containing 20% glycerol, 0.05% Tween 20, and 1 mM

EDTA, was found to be 163 μM, indicating that cholesterol does not form a strong complex with HPCD under the experimental conditions used. If so, according to the literature data on the release of weakly to moderately bound lipophiles from the cyclodexrtrin complexes (*24*), cholesterol should quantitatively dissociate in the assay buffer when its stock in HPCD is diluted 100-fold during titration experiments. It was also established that at least a 20-fold molar excess of HPCD over cholesterol is required to completely dissolve the substrate. To determine whether a higher molar ratio of HPCD/cholesterol in a stock solution of cholesterol in HPCD will affect cholesterol binding to CYP7A1, the enzyme was mixed with a fixed concentration of cholesterol and then titrated with increasing concentrations of HPCD. Two fixed concentrations of cholesterol at which the effect of HPCD was evaluated (5 and 20 μM) were selected on the basis of the range of cholesterol concentrations utilized for most of our K_d measurements. No decrease in $\Delta A_{390-420}$ induced by 20 and 5 μM cholesterol was observed up to 9000 and 2800 μM HPCD, respectively, indicating that cholesterol does not leave the P450 active site because HPCD does not compete with the enzyme for cholesterol at these concentrations. Thus, no more than a 450−560-fold molar excess of HPCD over cholesterol should be used in a stock solution to avoid its effect on cholesterol binding to the P450 in the spectral binding assay. For most of our titrations we used 10 mM cholesterol stock in 375 mM or 45% HPCD, and only two mutants, S285T and L485V, were titrated with 1 mM cholesterol because they had higher affinities for cholesterol. The binding constants of cholesterol for these mutants were essentially the same when titrations were carried out with 1 mM cholesterol in 37.5 mM HPCD and with 1 mM cholesterol in 375 mM HPCD, indicating that cholesterol availability to CYP7A1 does not seem to be affected even when the HPCD/cholesterol ratio is increased 10-fold and equal to 375.

Partially purified preparations of the wild-type and mutant enzymes with a specific heme content of 7−10 nmol/mg of protein and no more than 10% of the inactive P420 form were used. However, four of the mutants, L282A, W282F, S285T, and N288Q, contained ~50% of the P420 form.

Kinetic Studies with Cholesterol as a Substrate. The apparent K_m and k_{cat} values were determined as described (*20*) and analyzed with the Graph-Pad Prism software using the Michaelis−Menten equation. Cholesterol 7α-hydroxylase activity was assayed in 50 mM KP_i, pH 7.4, and 0.05% Tween 20 at 37 °C for 1−5 min. The reconstituted system (1 mL) contained P450 (0.01−1.0 μM), 1−100 units (0.5−50 μM) of rat NADPH−cytochrome P450 reductase, 2−200 μM cholesterol, 250000 cpm [1α,2α-^{3}H] cholesterol, 40 μg of L-dilauroylglyceryl-3-phosphocholine, and 1 mM NADPH. The product formation was linear with time and enzyme concentration and did not exceed 18% of total metabolism.

Enzyme Activity Measurements with Epicholesterol and 5-Androsten-3β-ol. Assay conditions were similar to those used for kinetic studies except a longer reaction time (10 min) and a fixed steroid concentration (50 μM) were used to maximize product formation. The concentration of P450 was 0.1 μM. To exclude that the product formation is the result of nonenzymatic oxidation with hydrogen peroxide, 0.25 μM (40 units) catalase was included in the assay. Reactions were terminated by adding 2 mL of CH_2Cl_2. Organic extracts were evaporated, converted into trimethylsilyl (TMSi) ethers, and analyzed by gas chromatography−mass spectrometry (GC-MS) using a Hewlett-Packard 5973 quadropole instrument (Palo Alto, CA) equipped with a Hewlett-Packard 19891A-102 column (25 m × 200 μm) (*26*). At first, each product was characterized by the full mass spectrum. If the spectrum was identical to that of one of the synthetic compounds (the 7α- and 7β-hydroxy and 7-oxo products of epicholesterol and 5-androsten-3β-ol), the product formation was quantified by determining the peak area of the total ion tracing at *m*/*z* 458 (molecular ion) for epicholestrol − TMSi, *m*/*z* 456 (M − 90) for monooxygenated products of epicholesterol − TMSi, *m*/*z* 346 for 5-androsten-3β-ol − TMSi, *m*/*z* 344 for monooxygenated products of 5-androsten-3β-ol − TMSi, and *m*/*z* 360 for 7-oxo-5-androsten-3β-ol − TMSi.

Synthesis of 7-Oxygenated Products of Epicholesterol and 5-Androsten-3β-ol. The 7α- and 7β-hydroxylated isomers of epicholesterol and 5-androsten-3β-ol as well as the corresponding 7-oxy analogues were produced by allylic oxidation with soybean lipoxygenase and linoleic acid essentially as described previously for formation of the corresponding metabolites of cholesterol (*27*). Linoleic acid, 50 mg in 0.25 mL of ethanol, was dissolved in 50 mL of sodium borate buffer, pH 9.5, containing 0.37 g of KCl. The incubation time was 30 min, and oxygen gas was blown over the solution, which was kept at 37 °C. The steroid, 300 μg, was added in 300 μL of acetone. Three portions (100000 units each) of soybean lipoxygenase were then added at 10 min intervals with continuous stirring. The reaction was terminated by the addition of 200 mL of methanol after 30 min, followed by addition of water and extraction with diethyl ether. The extraction was performed without prior acidification, and the ether was evaporated in vacuo. Part of the extracted material was converted into trimethylsilyl ether and analyzed directly by GC-MS. As expected, all three allylic oxidation products of the two 3β-hydroxy-5-unsaturated steroids were present in the mixture and could easily be identified by their typical mass spectra (*28*−*30*). In case of oxidation of epicholesterol, the yield of 7-oxoepicholesterol was calculated to be 14.4% (based on the total ion current chromatogram obtained in the mass spectrometric analysis). This product had a mass spectrum similar to that of 3β-hydroxy-5-cholesten-7-one and was identified by the molecular peak at *m*/*z* 472 (M) (theoretical *m*/*z* for $C_{30}H_{52}O_2Si$ 472.37) and peaks at *m*/*z* 457 (M − 15) and *m*/*z* 129 (characteristic for the Δ^5-3-trimethylsilyl ether group) (*29*, *30*). The two epimeric 7-hydroxylated products had been formed in a yield of 6.4% with a ratio of 1.7 between the two epimers (epimer with shortest retention time/epimer with the longest retention time). The mass spectra of the two epimers were almost identical with a dominating peak at *m*/*z* 456 (M − 90) due to facile elimination of the allylic thrimethylsilyloxy group at C7 (theoretical *m*/*z* for the molecular peak $C_{33}H_{62}O_2Si_2$ 546.43) as well as a peak at *m*/*z* 129 (*28*, *29*). The isomer with the shortest retention time was regarded to be the 7α isomer based on the finding that the 7α-hydroxy/7β-hydroxy isomers of cholesterol, dehydroepiandrosterone, and pregnenolone behave similarly in the same gas chromatography. Further evidence that the 7β isomer was the one with longest retention time was obtained by reduction of the mixture with sodium borohydride, which

```
102A1 4   -TIKEMPQPKTFGELKNLPLLNTDKPVQALMKIADELGEIFKFEAPGRVTRYLSSQRLIKEACDESRFDKNLSQA 77
2C5   12  -----PPGPTPFPIIGNILQIDAKDISKSLTKFSECYGPVFTVYLGMKPTVVLHGYEAVKEALV-DLGEEFAGRG 80
M51   1   MSAVALPRVSGGHDEHGHLEEFRTDPIGLMQRVRDECGDVGTFQLAGKQVVLLSGSHANEFFFR-------AGDD 68
7A1   33  -------LENGLIPYLGCALQFGANPLEFLRANQRKHGHVFTCKLMGKYVHFITNPLSYHKVLC---HGKY---- 93
                                      A Helix     β1-1    β1-1   B Helix

102A1 LKFVRDFAGDGLFTSWTHEKNWKKAHNILLPSF--SQQA---MKGYHAMMVDIAVQLV-QKWERLN------ADEH 141
2C5   SVPILEKVSKGLGIAFSNAKTWKEMRRFSLMTL--RNFG---MGKRSIEDRIQEEARCLVEELRKT------NASP 145
M51   DLDQAKAYPFMTPIFGEGVVFDASPERRKEMLH--NAAL---RGEQMKGHAATIEDQVRRMIADWG------EAGE 133
7A1   -------------------FDWKKFHFATSAKAFGHRSIDPMDGNTTENINDTFIKTL--QGHALNSLTESMMENL 148
       B′ Helix          C Helix                       D Helix

102A1 IEVPEDMTRLTLDTIGLCGFNY-RFN---SFYRDQPHPFITSMVRALDEAMNKLQRA 194
2C5   CDPTFILGCAPCNVICSVIFHN-RFDYKDEEFLKLMESLHENVELLGTPWLQVYNNF 201
M51   IDLLDFFAELTIYTSSACLIGK---------KFRDQLDGRFAKLYHELERGTDPLAY 181
7A1   QRIMRPPVSSNSKTAAWVTEGMYSFCYRVMFEAGYLTIFGRDLTRRDTQKAHILNNL 205
         E Helix                   F Helix

102A1 NPDDPAYDENKRQFQEDIKVMND--LVDKIIADRK----ASGEQSDDLLTHMLNGKDPETGEPL 252
2C5   PALLDYFPGIHKTLLKNADYIKNFIMEKVKEHQKL----LDVNNPRDFIDCFLIKMEQENNLEF 261
M51   VDPYLPIESFRRRDEARNGLVALVADIMNGRIANP----PTDKSDRDMLDVLIAVKAETGTPRF 241
7A1   DNFKQFDKVFPALVAGLPIHMFRTAHNAREKLAESLRHENLQKRESISELISLRMFLNDTLSTF 269
                  G Helix                          H Helix

102A1 DDENIRYQIITFLIAGHETTSGLLSFALYFLVKNPHVLQKAAEEAARVLVD--PVPSYKQVK---------QLKYVGMVLNEALRLW 328
2C5   TLESLVIAVSDLFGAGTETTSTTLRYSLLLLLKHPEVAARVQEEIERVIGR--HRSPCMQDRS--------RMPYTDAVIHEIQRFI 338
M51   SADEITGMFISMMFAGHHTSSGTASWTLIELMRHRDAYAAVIDELDELYGD--GRSVSFHALR--------QIPQLENVLKETLRLH 318
7A1   DDLEKAKTHLVVLWASQANTIPATFWSLFQMIRNPEAMKAATEEVKRTLENAGQKVSLEGNPICLSQAELNDLPVLDSIIKESLRLS 356
         I Helix                          J Helix          J′ Helix             K Helix

102A1 PTA-PAFSLYAKEDTVLG---GEYPLEKGDELMVLIPQLHRDKTIWGD--DVEEFRPERFENPSAI------- 388
2C5   DLLPTNLPHAVTRD-VRF---RNYFIPKGTDIITSLTSVLHDEKAFPNPKVFDP-GHFLDESGNFK------- 399
M51   PPL-IILMRVAKGE-FEV---QGHRIHEGDLVAASPAISNRIPEDFPDPHDFVPARYEQPRQEDLL------- 379
7A1   SAS--LNIRTAKEDFTLHLEDGSYNIRKDDIIALYPQLMHLDPEIYPDPLTFKYDRYLDENGKTKTTFYCNGLK 428
            β1-4   β2-4              K′ Helix

102A1 PQHAFKPFGNGQRACIGQQFALHEATLVLGMMLKHFDFE----DHTNYELDIKETLTLKPEGFVVKAKSKKIPLGG 460
2C5   KSDYFMPFSAGKRMCVGEGLARMELFLFLTSILQNFKLQSLVEPKDLDITAVVNGFVSVPPSYQLCFIPIHH---- 471
M51   NRWTWIPFGAGRHRCVGAAFAIMQIKAIFSVLLREYEFEM--AQPPESYRNDHSKMVVQLAQPACVRYRRRT---- 449
7A1   LKYYYMPFGSGATICPGRLFAIHEIKQFLILMLSYFELELIEGQAKCPPLDQSRAGLGILPPLNDIEFKYKFKHL- 503
                          helix L                        β4-1  β4-2    β4-3
```

FIGURE 1: Alignment of CYP7A1 with structurally characterized P450s 102A1 (PDB code 1JPZ), 2C5 (PDB code 1NR6), and MT51 (PDB code 1E9X) used for modeling. α-Helices and *β*-strands are underlined with single and double lines, respectively. Secondary structural elements of CYP7A1 were predicted using the program JPRED, and those of P450s 102A1, 2C5, and MT51 were taken from the PDB structures 1JPZ, 1NR6, and 1E9X, respectively. Residues implied in substrate or inhibitor binding by structural and our studies are in bold.

gave a preferential formation of the 7*β*-hydroxy isomer from 7-oxoepicholesterol. It is well established that reduction with sodium borohydride gives a preferential yield of the equatorial reduction product (*31*), which is the 7*β*-hydroxy isomer in case of 3*β*-hydroxy-5-unsaturated steroids. In case of allylic oxidation of 5-androsten-3*β*-ol, the 7-oxo product was formed in a yield of 18.4% with only traces of the two 7-hydroxylated products. 5-Androsten-3*β*-ol-7-one had the expected mass spectrum with a molecular peak at *m*/*z* 360 (theoretical *m*/*z* for $C_{22}H_{36}O_2Si$ 360.25) and a peak at *m*/*z* 129, and the two allylic products had a dominating peak at *m*/*z* 344 (M − 90, theoretical *m*/*z* for the molecular peak $C_{25}H_{46}O_2Si_2$ 434.3) as well as a peak at *m*/*z* 129. Treatment of the mixture with sodium borohydride converted most of the 7-oxo derivative into 5-androstene-3*β*,7*β*-diol, with very little formation of the 7α isomer.

RESULTS

Sequence Alignment and Model of CYP7A1. As described in Experimental Procedures, to construct a homology model of a protein, a sequence alignment must be generated of the query sequence with the templates (Figure 1). On aligning CYP7A1 with the template sequences of CYP2C5, CYP102A1, and CYP51, it was found that the region around the B′ helix seemed to be absent. Initially the ClustalW program alignment created a B′ helix region, but on visual inspection, it appeared from key residues and patterns that are present in eukaryotic-like P450 proteins that it was incorrect. That is, in the C helix of most eukaryotic P450s, there is the conserved pattern WcchR/H (where "c" is a charged residue and "h" is an uncharged residue). This pattern is seen in CYP7A1 as WKKFH which is very similar to the CYP2C5 template sequence of WKEMR, and the CYP102A1 eukaryotic-like sequence WKKAH, and to the CYP2B4 sequence of WRALR found in the C helix. (Note: CYP51 is a bacterial protein, and this conserved pattern is absent.) N-Terminal of the usual B′ helix between the A and B helices there is another common pattern which starts with a glycine at the end of the A helix and leads into *β* strands 1−1 and 1−2, which contain a *β*-turn. The *β*-strands are generally hydrophobic, and the *β*-turn, as shown in the sequence alignment in Figure 1, contains residues that are commonly found in turns such as glycine and proline in addition to a basic amino acid, either a lysine or an arginine.

Thus, with these conserved patterns at either end of the typical B′ helix region, it appears that there is no B′ helix region in CYP7A1. This has implications for the modeled structure in that the end of the substrate pocket is open with a portion of the heme exposed to solvent. This is the same region that is believed to be the access channel in CYP2C5, different from that found in CYP102A1 in which the access channel is between the F−G loop and the β-sheet 1. It is also a region that is commonly involved in substrate orientation in the substrate-binding pocket.

In addition to this atypical N-terminal alignment, there are several regions with additional residues in the more conserved C-terminal portion of the protein. One region is between the J′ helix and the K helix, and the other is between the meander region and the heme-binding loop. In the modeled structure, these insertion regions place additional loops pointing into solvent on the putative redox partner-binding side of the protein, also termed the proximal face, and are similar in sequence to CYP8A1 (prostacyclin synthase), which does not require a protein redox partner.

Cholesterol-Bound Model of CYP7A1. In the present study several cycles of model building and substrate docking were performed followed by site-directed mutagenesis to better understand the binding and orientation of the substrate in CYP7A1. Initially, residues to be mutated were selected on the basis of the ClustalW sequence alignment. Subsequently, when the adjusted alignment (as discussed above) and substrate-bound model were constructed, additional mutations in CYP7A1 were made. Those residues chosen along with substrate-contact residues in structurally characterized P450s are shown in Figure 1.

With the model of CYP7A1, the substrate was docked using three different methods: manual docking followed by molecular dynamics simulation, by the program Affinity, or by the HEX program, all giving similar results. When manually docking, the substrate was orientated such that the active α-hydrogen of the C7 carbon was placed in close proximity (approximately 2 Å) to the putative ferryl oxygen of the heme. Only two orientations of the substrate were possible because of steric hindrance. One of these orientations correlated with the initial mutagenesis data and, thus, was used as the preferred substrate-bound model for choosing the next set of residues to be mutated. After the second set of mutants was constructed and characterized, the cholesterol-bound model of CYP7A1 was further refined using the more recent substrate-bound structure of CYP2C5 (1N6B) and the substrate-bound form of P450102A1 (1JPZ), along with CYP51, resulting in the binding pocket shown in Figure 2. The active site residues in this second model remained the same as those in the first model. Interestingly, the F−G loop was found to partially cover the opening resulting from the absence of the more typical B′ helix.

Interaction of Different Cholesterol Derivatives with Wild-Type CYP7A1. Substrate-binding and enzyme activity studies were carried out to ascertain the importance of the cholesterol hydroxyl group and the side chain interaction with CYP7A1. No spectral response was induced by 5-cholestene (contains no hydroxyl, Figure 3, Table 1). This steroid did not displace cholesterol from the CYP7A1 active site in the displacement assay and did not inhibit cholesterol binding at 20 μM concentration (equal to five K_d values of cholesterol to CYP7A1). Together, these data suggest the lack of 5-cholestene binding to CYP7A1 and the crucial role of the cholesterol hydroxyl group in the formation of the enzyme−substrate complex. CYP7A1 was then titrated with 3-keto-cholesterol (contains a keto group instead of the hydroxyl; Figure 3, Table 1). The K_d for 3-ketocholesterol was only 2.5-fold higher than that for cholesterol, indicating a minor contribution of the hydrogen atom of the hydroxyl group to bonding with CYP7A1. Quite surprisingly, epicholesterol, which differs from cholesterol by having the hydroxyl in the 3α position instead of the 3β position (Figure 3), was also found to induce a spectral response in CYP7A1, although at a much lesser extent than did cholesterol (Table 1). Despite a 4-fold decreased ΔA_{max}, the K_d value was only 2.1 times higher than that for cholesterol. Reconstitution of catalytic activity with epicholesterol as a substrate followed by the GC-MS analysis of the enzyme assay extract revealed that this cholesterol derivative binds in several different orientations in the enzyme active site because three distinct product peaks (designated as P1, P2, and P3 in Figure 4A) were seen during the gas chromatography separation. The small peak in the tracing of the ion at *m*/*z* 456 preceding P1 in Figure 4A is a nonhydroxylated contaminant in the material incubated corresponding to a 3-hydroxylated C27 steroid with two double bonds. The amounts of P1, P2, and P3 corresponded to the conversion of about 0.5%, 1%, and 2% of the substrate, respectively, as quantified by the total ion tracing in the mass spectrometric analyses, with catalase having no effect on the rate of product formation. In a parallel incubation with cholesterol, the rate of product formation (7α-hydroxycholesterol) was much higher, 38%, indicating that CYP7A1 metabolizes epicholesterol much slower than

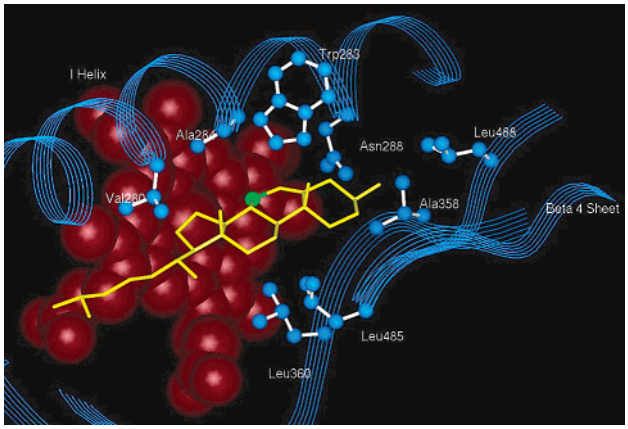

FIGURE 2: Substrate-binding pocket of CYP7A1. Cholesterol is in yellow, C7 of cholesterol is in green, and heme is in red.

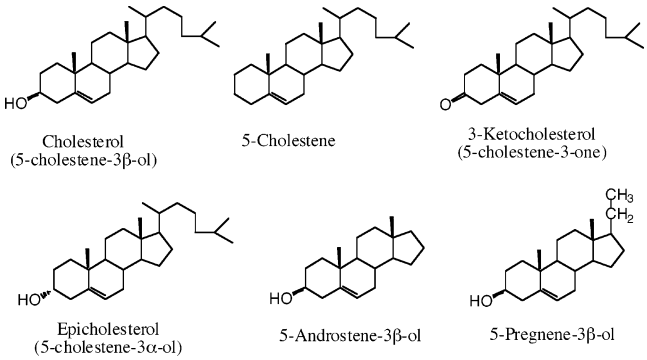

FIGURE 3: Chemical structures of compounds used in the present study.

Table 1: Binding of Different Cholesterol Derivatives to Wild-Type CYP7A1

derivative	K_d, μM[a]	ΔA_{max}[b]	cholesterol displacement[c]	inhibition of cholesterol binding[d]
cholesterol	4.3 ± 0.01	0.04 ± 0.006		
5-cholestene	no detectable spectral response[e]		no	no
3-ketocholesterol	10.8 ± 0.9	0.05 ± 0.002		
epicholesterol	8.7 ± 1.5	0.01 ± 0.001		
5-cholesten-3β-ol methyl ether	no detectable spectral response		no	no
cholesterol sulfate	no detectable spectral response		no	no
5-androsten-3β-ol	13.3 ± 2.5	0.005 ± 0.001		
5-pregnen-3β-ol	21.3 ± 0.4	0.016 ± 0.001		

[a] Calculated on the basis of the spectral binding assay as described under Experimental Procedures. The results represent the average of three different titrations ± SD. [b] Normalized to nanomoles of P450. [c] Assessed by the displacement assay as described under Experimental Procedures. [d] Assessed by the inhibition assay as described under Experimental Procedures. [e] The spectral response, $\Delta A_{390-420}$, was <0.002 absorbance units when 2 μM P450 was titrated with up to a 100 μM steroid.

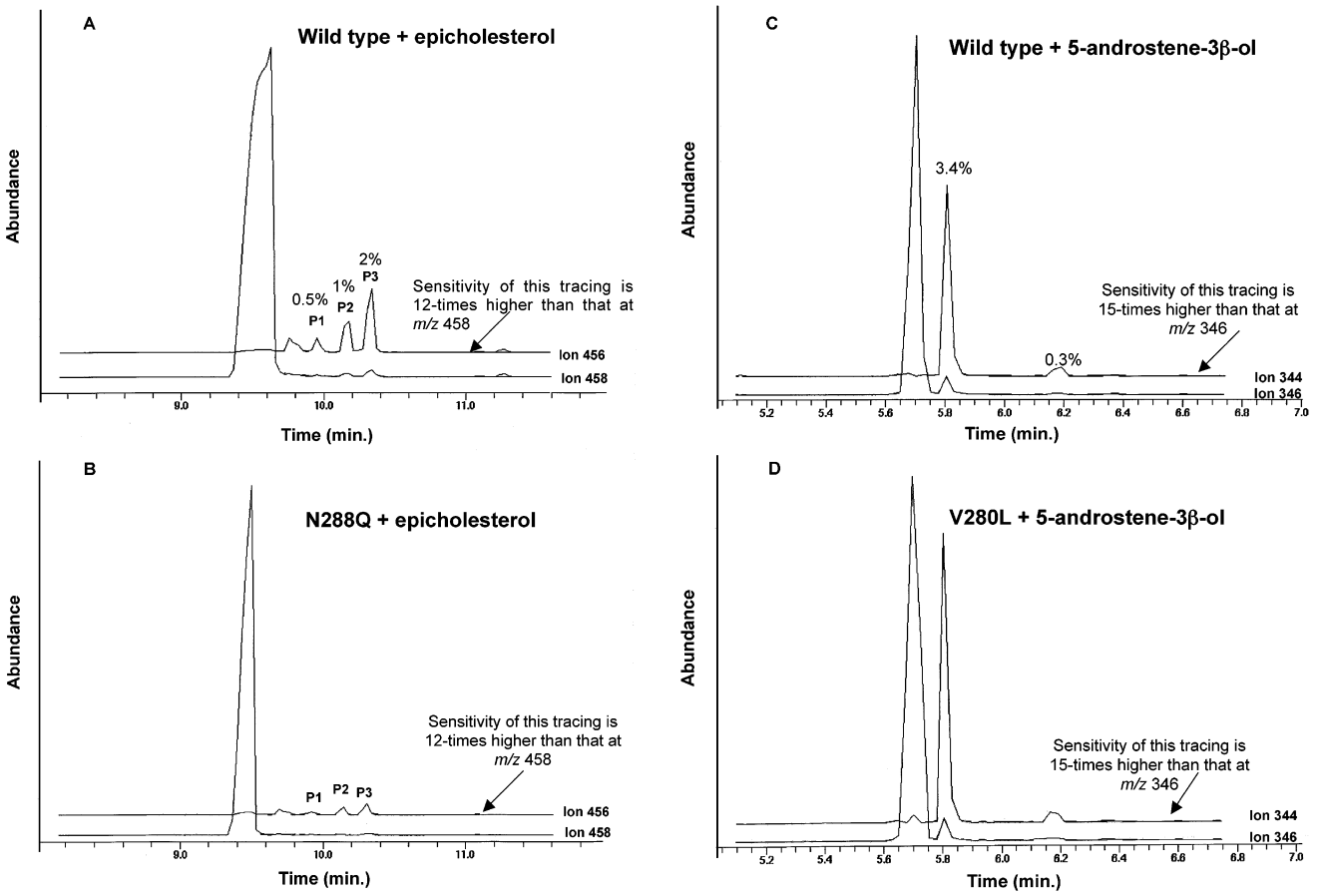

FIGURE 4: GS-MS analyses of the incubations of the wild-type CYP7A1 (A) and the N288Q mutant (B) with epicholesterol and the wild-type CYP7A1 (C) and the V280L mutant (D) with 5-androsten-3β-ol. In panels A and B, the trimethylsilyl ether of epicholesterol was recorded at *m*/*z* 458 (molecular ion) and trimethylsilyl ethers of monohydroxylated epicholesterol species at *m*/*z* 456 (M − 90). In panels C and D, the trimethylsilyl ether of 5-androsten-3β-ol was recorded at *m*/*z* 346 (molecular ion) and the trimethylsilyl ether of monohydroxylated products of 5-androsten-3β-ol at *m*/*z* 344 (M-90). Due to a difference in fragmentation intensity, the sensitivity in the detection of the 7-oxygenated products at *m*/*z* 456 (A and B) and *m*/*z* 344 (C and D) is between 12 and 15 times higher than that in the detection of the substrate at *m*/*z* 458 (A and B) and at *m*/*z* 346 (C and D).

cholesterol. The major product P3 in Figure 4A had the same mass spectrum and retention time as synthetic 5-cholestene-3α,7α-diol. The other minor products P1 and P2 were monohydroxylated species of epicholesterol. The position of the extra hydroxyl group in P1 was not clarified, whereas P2 contained the extra hydroxyl group in the nucleus: its mass spectrum had a fragment at *m*/*z* 253 and at *m*/*z* 343 (loss of an intact steroid side chain from *m*/*z* 456). None of the products in the incubations of CYP7A1 with epicholesterol were identical to 5-cholestene-3α,7β-diol. Thus, taken together, data on 5-cholestene, 3-ketocholesterol, and epicholesterol indicate that while CYP7A1 does not appear to have strict requirements for the stereochemistry of the hydroxyl at C3, it still requires a polar group at this position.

Spatial constraints in the active site around the 3β-OH were probed with 5-cholesten-3β-ol methyl ether and cholesterol sulfate (Table 1). Neither of the two steroids produced a detectable spectral response, displaced cholesterol from the CYP7A1 active site, and inhibited cholesterol binding. As with 5-cholestene, these data suggest a lack of

binding and space limitations around C3. The role of the cholesterol side chain was assessed by titrations with 5-androsten-3β-ol (contains no side chain; Figure 3) and 5-pregnen-3β-ol (contains a truncated side chain; Figure 3). The K_d values for 5-androsten-3β-ol and 5-pregnen-3β-ol were only 3.1- and 5-fold higher than that for cholesterol, respectively (Table 1), indicating weak nonpolar contacts of the cholesterol side chain with hydrophobic residues from the enzyme. A slightly lower affinity for 5-pregnen-3β-ol, which has a part of the side chain preserved, may reflect a different conformation of this truncated side chain compared with that in cholesterol. The side chain also seems to be required for effective displacement of water from the heme iron as judged by an 8- and 2.5-fold lower ΔA_{max} for 5-androsten-3β-ol and 5-pregnen-3β-ol, respectively. As is described in the next section, many of the CYP7A1 mutants that had significantly decreased ΔA_{max} had also significantly decreased k_{cat}, suggesting that increased hydration of the heme iron slows down the catalysis. Enzyme activity studies indicate that although the side chain contributes only moderately to the strength of interaction with CYP7A1, this functionality is important for positioning the cholesterol molecule inside the active site to allow 7α-hydroxylation. The GC-MS analysis of a silylated extract obtained after the fully reconstituted system with wild-type CYP7A1 was incubated with 5-androsten-3β-ol showed the presence of one major and one minor hydroxylated product in a yield of about 3.4% and 0.3%, respectively, calculated from the tracings of the total ions (Figure 4C). The two monohydroxylated products had the same retention time and mass spectrum as synthetic 5-androstene-3β,7α-diol and 5-androstene-3β,7β-diol, respectively. Since both the 7α- and the 7β-hydroxylated isomers are formed by autoxidation of the substrate, it was important to exclude the possibility that part of it may have been formed by autoxidation. In control incubations lacking P450, P450 reductase, or NADPH there was no significant conversion to the 7β-hydroxylated product, and the maximal conversion into the 7α-hydroxylated product was 0.1%. Inclusion of catalase in the assay mixture did not eliminate the product formation but resulted in even more product formed: both 7α- and 7β-hydroxylase activities were stimulated about 1.2−1.3-fold. It should be emphasized that, in order to avoid higher blank readings, the commercial substrate had to be purified by HPLC just before the incubations.

Substrate-Binding Properties of the Mutant P450s. A total of 41 mutants encompassing 26 amino acid residues were generated and characterized (Tables 2 and 3). Usually one nonconservative substitution was created for a residue that did not seem to be involved in the interaction with cholesterol according to the model or alignment, whereas two preferably conservative substitutions to a smaller and larger sized side chain were introduced when the residue in question was suggested by the model to point inside the active site. On the basis of how mutations affected spectral binding of cholesterol, amino acid residues could be arbitrarily placed into two groups. The first group includes residues 120, 357, 359, 361, 362, 363, 364, 473, 481, 483, 487, and 488 (the T120S, S357A, S359A, N361Q, N361L, I362L, R363L, T364V, A473V, S481A, A483V, I487L, I487V, L488V, and L488I mutants) whose replacements resulted in insignificant (≤2.3-fold) change of parameters of spectral binding. The 2.3-fold value was chosen as a cutoff limit for this group because disruption of an interaction involving nonpolar groups of a substrate and the protein weakens the free energy of binding, ΔG, by at least 0.5 kcal/mol, which corresponds to a 2.3-fold increase of K_d (*32*). Thus, 12 residues of 26 studied are unlikely to participate in contacts with cholesterol.

The second group is formed by residues 280, 281, 282, 283, 284, 285, 286, 287, 288, 358, 360, 480, and 485. Most of these were investigated by generating two mutations, and at least one of them induced either moderate (≥2.3-fold increase of K_d) or dramatic change of spectral binding properties (significantly reduced ΔA_{max} or the lack of spectral response or reverse type I spectral response). Residues of this second group could be divided into three subgroups based on location in the primary sequence: 280−288 (the putative helix I), 358−361 (the region between the K helix and β1−4), and 480−485 (the β4-sheet region).

Four side chains point inside the active site from the putative I helix according to the model with Val280 interacting with the cholesterol side chain, Ala284 being close to C18 at the C/D ring junction, Trp283 laying over C19 at the A/B ring junction, and Asn288 interacting with the 3β-hydroxyl (Figure 2). Mutation of Val280 to a smaller size Ala did not affect K_d as judged by the spectral or filter assays, whereas the larger size V280L, A284V, A284C, and N288Q mutations abolished a cholesterol-induced spectral response. To clarify whether a lack of a spectral response indicates a lack of cholesterol binding, the filter assay was employed. Much less, 2.6−5.9-fold, or only 17%−38% of cholesterol bound to the wild-type P450 was found to bind to the V280L, A284V, A284C, and N288Q mutants, and this cholesterol binding was in an unproductive orientation because there was no cholesterol hydroxylation when enzyme activity was measured. Studies with cholesterol analogues have established that there are at least two functionalities in the active site of wild-type CYP7A1, one that interacts with the steroid 3β-hydroxyl and another that hydrogen bonds with the 3α-hydroxyl. On the basis of the similar K_d values of cholesterol and epicholesterol for the wild-type CYP7A1 (Table 1), interactions with the 3α- and 3β-hydroxyls are of an equal strength. Thus, binding to the V280L, A284V, A284C, and N288Q mutants with the K_d similar to that of a wild-type P450 could be the result of cholesterol interaction with the functionality that in the wild-type enzyme forms a hydrogen bond with the 3α-hydroxyl. If so, binding will be in a 180° flipped orientation that could be unproductive and that leads to no spectral response. To test whether unproductive cholesterol orientation is due to a reduced volume of the active site, the V280L and A284C mutants were titrated with the smaller 5-pregnen-3β-ol and 5-androsten-3β-ol and found to interact with these steroids with apparent binding constants either similar to or ∼3-fold higher than those of the wild type or the V280A mutant (Table 3). This gain of function was also confirmed in the enzyme activity studies with the V280L mutant. This P450 was inactive in cholesterol 7α-hydroxylation but was able to 7α-hydroxylate 5-androsten-3β-ol (Figure 4D). There was also a small amount of 7β-hydroxylation by this mutant. Both products were also formed in the presence of catalase. Together, the binding and activity data indicate that the additional volume of the Leu side chain may exclude the cholesterol from the active site because of its interference with the cholesterol side chain,

Table 2: Cholesterol Binding and Kinetic Properties of CYP7A1 Wild Type and Mutants[a]

CYP7A1	spectral assay K_d, μM	spectral assay ΔA_{max}	filter assay, bound cholesterol, K_d, μM	filter assay, bound cholesterol, cpm[b]	K_m, μM	k_{cat}, min^{-1}	location in model/suggested role
wild type	4.3 ± 0.1	0.04 ± 0.006	8.2 ± 0.2	17502	7.0 ± 1.0	143.7 ± 18.6	
Residues Whose Mutations Resulted in Insignificant (≤2.3-fold) Change of Parameters of Spectral Binding							
T120S	4.4 ± 0.3	0.07 ± 0.009			ND[c]	ND	
S357A	2.7 ± 0.2	0.09 ± 0.002			ND	ND	
S359A	4.2 ± 0.3	0.08 ± 0.009			ND	ND	
N361Q	2.9 ± 0.8	0.08 ± 0.009			ND	ND	
N361L	3.5 ± 0.2	0.07 ± 0.004			ND	ND	
I362L	1.9 ± 0.2	0.02 ± 0.007			ND	ND	
R363L	6.3 ± 0.3	0.03 ± 0.002			ND	ND	
T364V	5.6 ± 0.3	0.06 ± 0.005			ND	ND	
A473V	6.9 ± 1.0	0.01 ± 0.001			ND	ND	
S481A	7.6 ± 0.5	0.02 ± 0.002			ND	ND	
A483V	4.7 ± 0.2	0.05 ± 0.001			ND	ND	
I487L	4.4 ± 0.3	0.04 ± 0.002			ND	ND	
I487V	7.3 ± 0.5	0.05 ± 0.002			ND	ND	
L488V	9.4 ± 0.7	0.03 ± 0.002			ND	ND	
L488I	4.1 ± 0.8	0.02 ± 0.002			ND	ND	
Residues with at least One Mutation That Affected Parameters of Spectral Binding either Moderately or Significantly							
Putative Helix I							
V280L	no spectral response[d]		14.1 ± 0.7	2915 (17)	no activity[e]		inside the active site near cholesterol side chain,
V280A	4.0 ± 0.5	0.008 ± 0.001	8.4 ± 0.6	12960 (74)	26.1 ± 2.7	29.5 ± 4.1	defines the size of the active site
V281L	3.3 ± 0.3	0.08 ± 0.004			12.6 ± 1.4	103.6 ± 2.5	
V281A	13.0 ± 1.8	0.03 ± 0.001			10.7 ± 0.3	8.6 ± 0.1	points away from the active site
L282A	no spectral response		6.9 ± 0.1	6368 (36)	no activity		points away from the active site toward the E helix
W283F	no spectral response		7.5 ± 0.4	2007 (12)	no activity		inside the active site, interacts with cholesterol
W283Y	11.7 ± 1.5	0.02 ± 0.002			31.4 ± 2.2	100.3 ± 14.0	C19 methyl
A284V	no spectral response				no activity		inside the active site pointing toward pyrrole
A284C	no spectral response		6.9 ± 0.4	2893 (17)	no activity		ring B of the heme
S285A	4.6 ± 0.8	0.07 ± 0.007			ND	ND	points away from the active site
S285T (rt I)[f]	0.1 ± 0.03	0.15 ± 0.03	0.4 ± 0.05	2632 (15)	16.6 ± 2.0	7.3 ± 0.6	
Q286N	7.5 ± 0.7	0.05 ± 0.001			ND	ND	points away from the active site
Q286M	1.5 ± 1.3	0.007 ± 0.001	6.2 ± 0.2	611 (4)	32.0 ± 4.1	105.2 ± 12.3	
A287V	4.4 ± 1.0	0.006 ± 0.001			4.6 ± 0.5	9.8 ± 1.5	points away from the active site
A287C	3.8 ± 0.6	0.007 ± 0.001	3.1 ± 0.3	836 (5)	24.7 ± 5.6	10.1 ± 2.3	
N288Q	no spectral response		4.5 ± 0.4	6573 (38)	no activity		inside the active site, interacts with cholesterol
N288L	inactive P420 protein						3β-hydroxyl
Putative Helix K−β1−4 Region							
A358V	32.5 ± 2.5	0.02 ± 0.002			25.1 ± 3.8	3.8 ± 0.5	inside the active site near cholesterol C3,
					additional products		defines the size of the active site
L360I	2.5 ± 0.2	0.04 ± 0.003			14.9 ± 1.4	127.6 ± 8.2	inside the active site, interacts with cholesterol
L360V	14.8 ± 2.1	0.04 ± 0.004			17.7 ± 3.4	98.7 ± 3.7	C18 methyl
Putative β4 Sheet Region							
Q480N	12.6 ± 0.8	0.03 ± 0.002			8.8 ± 1.1	39.7 ± 2.5	points away from the active site, solvent
Q480M	7.9 ± 0.1	0.03 ± 0.004			ND	ND	exposed
R482L	inactive P420 protein						points away from the active site
L485V (rt I)	0.98 ± 0.3	0.01 ± 0.001	0.9 ± 0.1	766 (4)	12.5 ± 3.3	16.9 ± 3.3	inside the active site near cholesterol B/C ring
L485I	12.7 ± 2.2	0.02 ± 0.004			23.5 ± 2.2	4.6 ± 0.4	junction, defines the size of the active site

[a] Both kinetic and binding results represent the average of three independent experiments ± SD. ΔA_{max} in the spectral assay is normalized to nanomoles of P450. [b] Represents specific binding, i.e., radioactivity that was displaced with cold cholesterol at saturating concentrations. Nonspecific cholesterol binding to wild-type CYP7A1 was 15%. Number in parentheses shows percent of cholesterol binding compared with that to the wild-type enzyme. [c] ND, not determined. [d] The spectral response, $\Delta A_{390-420}$, was <0.002 absorbance units when 2 μM P450 was titrated with up to a 100 μM steroid. [e] Indicates k_{cat} < 0.2 min^{-1}. [f] rt I, reverse type I spectral response.

whereas the alternate substrates having a shorter steroid side chain or lacking the side chain could be appropriately orientated and metabolized. Thus, Val280 and Ala284 seem to play a role both in orientation and in specificity of substrate by controlling the volume of the active site.

Mutation of Trp283 to a smaller Tyr resulted in a 2.7-fold increase of K_d for cholesterol, whereas the Phe substitution abolished the cholesterol-induced spectral response. These data are in agreement with the homology model which suggests that position 283 in CYP7A1 should be occupied by a large residue that possibly acts as a lid to keep the cholesterol near the heme. The cholesterol side chain does not seem to be involved in the interaction with Trp283 as judged by essentially the same affinity of the W283Y mutant for 5-pregnen-3β-ol and an even stronger affinity for 5-androsten-3β-ol. The homology model suggests that Asn288 interacts with the cholesterol 3β-hydroxyl either directly or through the water molecule. Our spectral, filter, and enzyme activity data showing that Asn288 is essential for binding of cholesterol in correct orientation inside the enzyme active site support this suggestion. Titrations with cholesterol analogues established that the N288Q mutant interacts with

Table 3: Binding of Different Cholesterol Derivatives to the CYP7A1 Mutants[a]

	cholesterol		5-pregnen-3β-ol		5-androsten-3β-ol		epicholesterol		3-ketocholesterol	
form	K_d, μM	ΔA_{max}	K_d, μM	ΔA_{max}	K_d, μM	ΔA_{max}	K_d, μM	ΔA_{max}	K_d, μM	ΔA_{max}
WT	4.3 ± 0.01	0.04 ± 0.006	21.3 ± 0.4	0.016 ± 0.001	13.3 ± 2.5	0.005 ± 0.0004	8.7 ± 1.5	0.01 ± 0.001	10.8 ± 0.9	0.05 ± 0.002
V280L	no spectral response[b]		18.6 ± 2.4	0.007 ± 0.001	15.5 ± 1.5	0.005 ± 0.0001				
V280A	4.0 ± 0.5	0.01 ± 0.001	14.1 ± 0.6	0.003 ± 0.0001	4.9 ± 0.3	0.001 ± 0.0002				
W283Y	11.7 ± 1.5	0.02 ± 0.002	15.0 ± 2.0	0.004 ± 0.0001	2.2 ± 0.2	0.001 ± 0.0001				
W283F	no spectral response		no spectral response		no spectral response					
A284C	no spectral response		18.9 ± 0.1	0.003 ± 0.0005	40.8 ± 3.3	0.005 ± 0.0005				
N288Q	no spectral response						7.8 ± 1.3	0.05 ± 0.005	18.2 ± 0.3	0.01 ± 0.001
A358V	32.5 ± 2.5	0.02 ± 0.002					no spectral response		9.4 ± 0.4	0.04 ± 0.002

[a] Calculated on the basis of the spectral binding assay as described under Experimental Procedures. The results represent the average of three different titrations ± SD. [b] The spectral response, $\Delta A_{390-420}$, was <0.002 absorbance units when 2 μM P450 was titrated with up to a 100 μM steroid.

a smaller 3-ketocholesterol and epicholesterol (Table 3). These data indicate that, as in the case with Val280 and Ala284, a reduction of the volume of the active site could also be the reason for the altered cholesterol orientation in the N288Q mutant. Studies with epicholesterol also suggest that Asn288 does not interact with the steroid 3α-hydroxyl group. This interpretation is in agreement with the GC-MS analysis of the incubations of the N288Q mutant with epicholesterol showing the formation of the same products as those observed in the incubations with the wild-type enzyme (Figure 4A,B), although at a much lower rate. Both the spectral and enzyme activity data suggest that epicholesterol binds to the active site of the N288Q mutant and the wild-type enzyme in the same orientation, which, however, is different from that of cholesterol. Asn288 also appears to be involved in the stability of the protein, possibly by a hydrogen bond network that maintains a proper protein folding since the N288L mutation resulted in the inactive P420 enzyme. One more replacement in the putative I helix dramatically affected the mode of cholesterol interaction with CYP7A1. The S285T mutant exhibited a reverse type I spectral response with a peak at 421 nm and a trough at 388 nm, and the spectral K_d 43 times lower than that of the wild-type enzyme. Much tighter cholesterol binding was also confirmed by the filter assay. According to the model, the side chain of Ser285 points toward the E helix, away from the substrate-binding pocket. The effect of the S285T mutation could be due to a conformational change induced by a large size substitution. This interpretation is supported by the S285A mutation that did change the spectral K_d for cholesterol.

Only two side chains, Ala358 and Leu360, were implicated by site-directed mutagenesis and homology modeling to point inside the active site in the region between the putative helix K and the β1−4 sheet and assist in orientation and positioning of cholesterol. The A358V mutation caused a 7.6-fold increase in the spectral K_d for cholesterol. This deterioration of the affinity could be explained by a limited space around C3 in the active site with a larger size A358V substitution pushing the cholesterol 3β-hydroxyl away from the position that is optimal for formation of a stable interaction with Asn288, either directly or through a water molecule. The ability of the A358V mutant to interact with the smaller 3-ketocholesterol, which is approximately 1.5 Å narrower around the C3 of the steroid A ring than either the epicholesterol or cholesterol, supports this interpretation and suggests that position 358 in CYP7A1 should be occupied by a small residue to provide enough space in the active site for cholesterol to bind. No spectral response was observed upon the titration of the A358V mutant with epicholesterol. The enzyme was also inactive in epicholesterol hydroxylation as assessed by GC-MS. These data, which are concordant with the homology model, indicate that epicholesterol may be unable to properly dock into the active site in the A358V mutant because of steric hindrance between the 3α group and the bulkier valine resulting in the lack of spectral shift and turnover. For Leu360, the homology model suggests that this side chain could be involved in positioning the cholesterol appropriate for hydroxylation, and in the L360V mutant, the smaller side chain may allow a lateral displacement of the cholesterol, causing a decreased affinity for the correct substrate orientation. The site-directed mutagenesis data are in agreement with this notion: the L360V replacement resulted in a 3.4-fold increase of the spectral K_d for cholesterol, whereas the L360I substitution did not affect cholesterol binding, indicating that Leu360 contacts the cholesterol C18 methyl group through its terminal side chain carbon which is preserved when Leu is substituted with Ile.

The last two residues whose mutations affected cholesterol affinity either moderately (Gln480) or dramatically (Leu485) were found in the β4-sheet region. Conservative replacement of Gln480 with a smaller Asn resulted in a 2.9-fold increase of the spectral K_d, whereas the nonconservative substitution of Met having a similar length increased K_d only 1.8-fold. The observed effects suggest some size requirements for position 480 and could be due to tertiary conformational changes because Gln480 points away from the active site in the model. Leu485, in contrast, points inside the active site in the model defining its volume over the cholesterol B/C ring junction. Replacement with a smaller Val led to a reverse type I spectral response and a tighter (4−8-fold) cholesterol binding based on both spectral and filter assays. Substitution with the same size Ile had an opposite effect, resulting in type I spectral response and a 3 times looser cholesterol binding. Comparison of the two mutations indicates very strict requirements for the size and structure of the residue at position 480 for optimum orientation of cholesterol.

Kinetic Properties of the Mutant P450s 7A1. Mutants with moderate and significant changes of cholesterol binding properties, as well as those exhibiting reverse type I spectral response or significantly reduced (>6-fold) ΔA_{max}, were assayed for cholesterol 7α-hydroxylase activity, and the kinetic parameters were determined, if product formation was observed (Table 2). Of the 20 mutants examined, six (V280L, L282A, W283F, A284V, A284C, and N288Q) did not

metabolize cholesterol even when 50 times higher amounts of P450 and high cholesterol concentrations (100 μM) were used in the reconstitution system and the reaction time was increased 10-fold. Also, none of these mutants exhibited cholesterol-induced spectral response. Three mutants, W283Y, Q286M, and L360V, had a 3−4.5-fold increased K_m and insignificantly altered k_{cat} (<1.6-fold). The increased K_m of the W283Y and L360V mutants is most likely the result of the increased K_d, whereas a change in the K_m of the Q286M mutant is probably due to the reduced amount of bound cholesterol as is indicated by the filter assay and supported by the reduced ΔA_{max} in the spectral assay. Three mutants, S285T, L485V, and A287V, had their K_m values changed insignificantly (<2.3-fold), while the k_{cat} values were decreased 8.5−20-fold. The decreased rates of catalysis likely reflect the increased solvation of the heme iron in these mutants as judged by the reverse type I cholesterol-induced spectral response exhibited by the S285T and L485V mutants and significantly decreased ΔA_{max} of the A287V mutant. Finally, three mutants, A287C, V280A, and A358V, had a 2.9−3.7-fold increased K_m and a 4.8−36-fold decreased k_{cat}. While both, Val and Cys, replacements at position 287 led to a significantly decreased k_{cat}, only the latter resulted in a 3.5-fold increase in K_m. Val and Cys both have a similar size, but Cys is a hydrogen donor and may form bonds, whereas Val cannot. It is possible that the Cys substitution introduced conformational changes through bonding to a nearby residue and thus altered the K_m. Although a simultaneous change of K_m and k_{cat} is always difficult to interpret, the kinetic properties of the V280A and A358V mutants are in agreement with our notion that Val280 and Ala358 are located inside the enzyme active site and important for proper cholesterol binding. The A358V substitution also caused an appearance of a new peak in the HPLC product profile in the amounts of 20%−25% of that of 7α-hydroxycholesterol (not shown). While an attempt to identify this product by GC-MS was not successful because too little of this unknown metabolite was produced, the GC-MS analysis did reveal the formation of 7β-hydroxycholesterol (α and β isomers of 7-hydroxycholesterol are not separated under our conditions of HPLC) in the amounts of 3%−10% of that of 7α-hydroxycholesterol and ruled out that 7β-hydroxycholesterol is the result of nonenzymatic cholesterol oxidation because the major autoxidation product of cholesterol, 7-oxocholesterol, was not detected.

DISCUSSION

Among four P450s that are known to initiate cholesterol degradation in humans, 7A1, 11A1, 27A1, and 46A1, the former has the highest catalytic efficiency of cholesterol hydroxylation in the reconstituted system in vitro (*33*−*35*), which, in our opinion, reflects physiological requirements for the liver to degrade about 600 mg of cholesterol on a daily basis (*36*). For comparison, about 40, 50, and 6−7 mg of cholesterol are hydroxylated every day by P450s 11A1, 27A1, and 46A1, respectively, in steroidogenic and extrahepatic tissues and the brain (*36*−*38*). The present work is a continuation of our studies aimed at establishing the features of the CYP7A1 molecule that result in the strict substrate specificity and high rate of catalysis.

Sequence alignment with structurally characterized P450s (Figure 1) and a homology model of CYP7A1 indicates that CYP7A1 contains extra loops on the proximal face, lacks the B′ helix, and contains Asn288 in the I helix instead of a highly conserved threonine which is thought to be required for dioxygen bond cleavage during catalysis (reviewed in ref *39*). These features produce a novel P450. Among structurally determined P450s, the B′ helix is absent in only bacterial P450cin, which also contains Asn instead of a conserved threonine (*40*). The extra loops are also seen in CYP8A1, which is an endoperoxidase not requiring an NAPDH reductase as a source of electrons. Additionally, with the lack of the B′ helix, the edge of the heme is partially exposed in the model. Thus, one might speculate that the site of CYP7A1/reductase interaction is novel compared to other already studied P450s.

While a thorough investigation of whether the B′ helix is indeed missing in the structure was not pursued herein, the role of Asn288 was assessed. Our data strongly suggest that Asn288 is a key residue for binding cholesterol because this side chain interacts with the steroid 3β-hydroxyl either directly or via a water molecule. Furthermore, as the N288L substitution that produced a denatured P420 protein indicates, Asn288 is also involved in a network responsible for maintaining a stable protein structure. This is in contrast to CYP101A1 (*41*), CYP1A2 (*42*), CYP102A1 (*43*), CYP2B4 (*44*), CYP3A4 (*45*), and P450nor (*46*), in which replacement of a conserved threonine with a residue that does not have a hydrogen-bonding capacity still results in a functionally folded enzyme. Thus, it would seem that Asn288 forms a stabilizing hydrogen bond network in the substrate-free protein, and in the presence of cholesterol, the C3 β-hydroxyl allows for an alternate network. In the N288Q mutant the increased length of the side chain may prevent cholesterol from docking appropriately in the active site and participating in the "new" hydrogen bond network, whereas the C3 α-hydroxy group in epicholesterol may allow for substrate binding and catalysis. A similar reason might be the case for binding and catalysis of 3-ketocholesterol. We hope to obtain more information about Asn288 in future by investigating how CYP7A1 hydroxylates epicholesterol. In addition to Asn288, six more residues are suggested to interact with cholesterol in our studies (Figure 2, Table 2), three in the putative I helix or *s*ubstrate *r*ecognition *s*ite 4, SRS-4 (Val280, Trp283, and Ala284), two in the helix K−β1−4 region or SRS-5 (Ala358 and Leu360), and one in the β4-sheet region or SRS-6 (Leu485). The SRS regions are those defined by Gotoh (*47*). These residues are aligned with determinants of substrate specificity in structurally characterized P450s (Figure 1), which is concordant with the notion that substrate-contact residues in different P450s are located at the same or similar alignment positions (*48*). Conservative, larger sized V280L, A284V, A284C, and N288Q substitutions of three active site residues in the putative I helix and a smaller size aromatic W283F mutation of the fourth side chain in this region resulted in cholesterol binding in an unproductive orientation. The smaller L485V replacement in the putative β4-sheet region caused a reversed type I spectral response and a much tighter cholesterol binding, whereas the very conservative L485I mutation did not change the type of the spectral response but led to a 3-fold looser substrate binding. These and the kinetic data indicate that the requirement for the size of the active site residue is also strict at position 485. The A358V substitution in the putative

helix K−β1−4 region preserved the type I spectral response but increased the spectral K_d for cholesterol 8-fold and resulted in a 37-fold decrease of k_{cat} and formation of two new products, one of which was not identified and 7β-hydroxycholesterol. Such properties of the mutant enzyme again suggest strict requirements for the size of a side chain at position 358 in CYP7A1. Only Leu360 in the helix K−β1−4 region could be mutated without significant functional consequences. Thus, our mutagenesis data indicate that there seems to be a very good complementarity of fit between the cholesterol molecule and the enzyme active site. This type of tight fit of substrate and enzyme active site in a P450 was initially observed for CYP101A1, a prokaryotic P450 which metabolizes camphor (reviewed in ref *39*). Subsequent studies established that this complementary fit is also true for some eukaryotic P450s from families 2, 3, and 4 (reviewed in refs *48* and *49*). This present work provides experimental evidence that the "complementarity" mechanism is also responsible for the strict substrate specificity of CYP7A1, possibly by reducing the rotational freedom of the substrate inside the enzyme active site and resulting in one binding orientation and a good coupling of the P450 reaction cycle as suggested for CYP101A1 (*39*).

A correlation between the hydration of the heme iron and the catalytic rate constant, k_{cat}, was also observed. Nine mutants had significantly (no less than 3.6-fold) decreased k_{cat}. Seven of them (A287V, A287C, V280A, V281A, A358V, Q480N, and L485I) exhibited a type I cholesterol-induced spectral response and a decreased ΔA_{max}, indicating that less water, than in the wild type enzyme, is displaced from the heme iron upon substrate binding. Two mutants (S285T and L485V) showed a reverse type I cholesterol-induced spectral response, indicating that substrate binding does not cause water displacement but, in contrast, leads to a higher percentage of protein molecules with water ligated to the heme iron. Thus, cholesterol-bound forms of all nine catalytically impaired mutants had increased solvation of the heme iron compared with that of cholesterol-bound wild type, but this increase in solvation was realized through two different mechanisms. Because seven of nine mutations with decreased k_{cat} were in the active site, it is also possible that precise substrate positioning, which is a key factor for tight coupling of P450 enzymatic reaction (reviewed in ref *39*), was also affected and contributed to a less productive catalysis. A pivotal role of water in efficient catalysis was demonstrated previously by crystallographic studies of a complex between P450 102A1 and the novel substrate *N*-palmitoylglycine (NPG) (*18*). NPG interacts with higher affinity and reacts with a higher turnover number than palmitic acid. It was established that NPG binding results in generation of the high-affinity water binding site converting the enzyme to a form with high catalytic competence likely because water displacement raises the reduction potential of the heme iron and, by making the iron easier to reduce, increases the efficiency of usage of reducing equivalents required for substrate hydroxylation (*18*). Our data indicate that CYP7A1 may be similar in this respect to P450 102A1.

To summarize, the present comprehensive investigation was aimed at understanding how CYP7A1, a key enzyme in cholesterol homeostasis in humans, binds cholesterol and is adapted to fit physiological requirements for a high rate of cholesterol turnover in the liver. Our previous studies indicate that strict substrate specificity of CYP7A1 is in part determined by the initial cholesterol recognition that takes place on the surface of the molecule (*20*). Herein, through computer modeling and site-directed mutagenesis, we gained insight into the CYP7A1 active site and identified two additional features that appear to contribute significantly to the enzyme strict substrate specificity and regio- and stereoselectivity of hydroxylation and high rate of catalysis. These features are a good complementarity fit between the cholesterol molecule and the enzyme active site and a requirement for displacing the water molecule from the heme iron upon substrate binding. The present work significantly advances our understanding of the molecular mechanisms of cholesterol binding and catalysis in mammals and serves as a paradigm for our ongoing studies of another three cholesterol-metabolizing P450s, CYP11A1, CYP27A1 and CYP46A1.

ACKNOWLEDGMENT

Oligonucleotide synthesis and DNA sequencing were carried out by the recombinant DNA Laboratory and the Protein Chemistry Laboratory, respectively, at the University of Texas Medical Branch.

SUPPORTING INFORMATION AVAILABLE

One table listing oligonucleotides used to generate CYP7A1 mutants. This material is available free of charge via the Internet at http://pubs.acs.org.

REFERENCES

1. Turley, S. D., and Dietschy, J. M. (1982) *The Liver: Biology and Pathobiology*, Raven Press, New York.
2. Myant, N. B., and Mitropoulos, K. A. (1977) Cholesterol 7a-hydroxylase, *J. Lipid Res. 18*, 135−153.
3. Ogishima, T., Deguch, S., and Okuda, K. (1987) Purification and characterization of cholesterol 7a-hydroxylase from rat liver microsomes, *J. Biol. Chem. 262*, 7646−7650.
4. Pullinger, C. R., Eng, C., Salen, G., Shefer, S., Batta, A. K., Erickson, S. K., Verhagen, A., Rivera, C. R., Mulvihill, S. J., Malloy, M. J., and Kane, J. P. (2002) Human cholesterol 7alpha-hydroxylase (CYP7A1) deficiency has a hypercholesterolemic phenotype, *J. Clin. Invest. 110*, 109−117.
5. Norlin, M., Andersson, U., Bjorkhem, I., and Wikvall, K. (2000) Oxysterol 7 alpha-hydroxylase activity by cholesterol 7 alpha-hydroxylase (CYP7A), *J. Biol. Chem. 275*, 34046−34053.
6. Norlin, M., Toll, A., Bjorkhem, I., and Wikvall, K. (2000) 24-Hydroxycholesterol is a substrate for hepatic cholesterol 7alpha-hydroxylase (CYP7A), *J. Lipid Res. 41*, 1629−1639.
7. Hasemann, C. A., Kurumbail, R. G., Boddupalli, S. S., Peterson, J. A., and Deisenhofer, J. (1995) Structure and function of cytochromes P450: a comparative analysis of three crystal structures, *Structure 3*, 41−62.
8. Graham-Lorence, S., Amarneh, B., White, R. E., Peterson, J. A., and Simpson, E. R. (1995) A three-dimensional model of aromatase cytochrome P450, *Protein Sci. 4*, 1065−1080.
9. Graham-Lorence, S., and Peterson, J. A. (1996) P450s: structural similarities and functional differences, *FASEB J. 10*, 206−214.
10. Peterson, J. A., and Graham, S. E. (1998) A close family resemblance: the importance of structure in understanding cytochromes P450, *Structure 6*, 1079−1085.
11. Graham, S. E., and Peterson, J. A. (1999) How similar are P450s and what can their differences teach us?, *Arch. Biochem. Biophys. 369*, 24−29.
12. Cosme, J., and Johnson, E. F. (2000) Engineering microsomal cytochrome P450 2C5 to be a soluble, monomeric enzyme. Mutations that alter aggregation, phospholipid dependence of catalysis, and membrane binding, *J. Biol. Chem. 275*, 2545−2553.
13. Ravichandran, K. G., Boddupalli, S. S., Hasermann, C. A., Peterson, J. A., and Deisenhofer, J. (1993) Crystal structure of

hemoprotein domain of P450BM-3, a prototype for microsomal P450's, *Science 261*, 731−736.
14. Richardson, T. H., and Johnson, E. F. (1994) Alterations of the regiospecificity of progesterone metabolism by the mutagenesis of two key amino acid residues in rabbit cytochrome P450 2C3v, *J. Biol. Chem. 269*, 23937−23943.
15. Poulos, T. L., Finzel, B. C., and Howard, A. J. (1987) High-resolution crystal structure of cytochrome P450cam, *J. Mol. Biol. 195*, 687−700.
16. Cupp-Vickery, J. R., and Poulos, T. L. (1995) Structure of cytochrome P450eryF involved in erythromycin biosynthesis, *Nat. Struct. Biol. 2*, 144−153.
17. Li, H., and Poulos, T. L. (1997) The structure of the cytochrome p450BM-3 haem domain complexed with the fatty acid substrate, palmitoleic acid, *Nat. Struct. Biol. 4*, 140−146.
18. Haines, D. C., Tomchick, D. R., Machius, M., and Peterson, J. A. (2001) Pivotal role of water in the mechanism of P450BM-3, *Biochemistry 40*, 13456−13465.
19. Wester, M. R., Johnson, E. F., Marques-Soares, C., Dijols, S., Dansette, P. M., Mansuy, D., and Stout, C. D. (2003) Structure of mammalian cytochrome P450 2C5 complexed with diclofenac at 2.1 Å resolution: evidence for an induced fit model of substrate binding, *Biochemistry 42*, 9335−9345.
20. Nakayama, K., Puchkaev, A., and Pikuleva, I. A. (2001) Membrane binding and substrate access merge in cytochrome P450 7A1, a key enzyme in degradation of cholesterol, *J. Biol. Chem. 276*, 31459−31465.
21. Omura, R., and Sato, R. (1964) The carbon monoxide-binding pigment of liver microsomes, *J. Biol. Chem. 239*, 2370−2378.
22. Guengerich, F. P., Miller, G. P., Hanna, I. H., Martin, M. V., Leger, S., Black, C., Chauret, N., Silva, J. M., Trimble, L. A., Yergey, J. A., and Nicoll-Griffith, D. A. (2002) Diversity in the oxidation of substrates by cytochrome P450 2D6: lack of an obligatory role of aspartate 301-substrate electrostatic bonding, *Biochemistry 41*, 11025−11034.
23. Pitha, J., Irie, T., Sklar, P. B., and Nye, J. S. (1988) Drug solubilizers to aid pharmacologists: amorphous cyclodextrin derivatives, *Life Sci. 43*, 493−502.
24. Stella, V. J., Rao, V. M., Zannou, E. A., and Zia, V. V. (1999) Mechanisms of drug release from cyclodextrin complexes, *Adv. Drug Deliv. Rev. 36*, 3−16.
25. Davydov, D. R., Kumar, S., and Halpert, J. R. (2002) Allosteric mechanisms in P450eryF probed with 1-pyrenebutanol, a novel fluorescent substrate, *Biochem. Biophys. Res. Commun. 294*, 806−812.
26. Bjorkhem, I., Andersson, U., Ellis, E., Alvelius, G., Ellegard, L., Diczfalusy, U., Sjovall, J., and Einarsson, C. (2001) From brain to bile. Evidence that conjugation and omega-hydroxylation are important for elimination of 24S-hydroxycholesterol (cerebrosterol) in humans, *J. Biol. Chem. 276*, 37004−37010.
27. Lund, E., Diczfalusy, U., and Bjorkhem, I. (1992) On the mechanism of oxidation of cholesterol at C-7 in a lipoxygenase system, *J. Biol. Chem. 267*, 12462−12467.
28. Brooks, C. J., Henderson, W., and Steel, G. (1973) The use of trimethylsilyl ethers in the characterization of natural sterols and steroid diols by gas chromatography−mass spectrometry, *Biochim. Biophys. Acta 296*, 431−445.
29. Breuer, O., and Bjorkhem, I. (1990) Simultaneous quantification of several cholesterol autoxidation and monohydroxylation products by isotope-dilution mass spectrometry, *Steroids 55*, 185−192.
30. Brooks, C. J. W., Horning, E. C., and Young, J. S. (1968) Characterization of sterols by gas chromatography−mass spectrometry of the trimethylsisyl ethers, *Lipids 3*, 391−402.
31. Djerassi, C. (1963) in *Steroid Reactions: An Outline for Organic Chemists*, pp 135−138, Holden-Day, San Francisco.
32. Fersht, A. R. (1987) The hydrogen bond in molecular recognition, *Trends Biochem. Sci. 12*, 301−304.
33. Murtazina, D., Puchkaev, A. V., Schein, C. H., Oezguen, N., Braun, W., Nanavati, A., and Pikuleva, I. A. (2002) Membrane-protein interactions contribute to efficient 27-hydroxylation of cholesterol by mitochondrial cytochrome P450 27A1, *J. Biol. Chem. 277*, 37582−37589.
34. Mast, N., Andersson, U., Nakayama, K., Bjorkhem, I., and Pikuleva, I. A. (2004) Expression of human cytochrome P450 46A1 in *Escherichia coli*: effects of N- and C-terminal modifications, *Arch. Biochem. Biophys. 428*, 99−108.
35. Pikuleva, I. A. (2004) Putative F−G loop is involved in association with the membrane in P450scc (P450 11A1), *Mol. Cell. Endocrinol. 215*, 161−164.
36. Sabine, J. R. (1977) *Cholesterol*, Marcel Dekker, New York and Basel.
37. Duane, W. C., and Javitt, N. B. (1999) 27-hydroxycholesterol: production rates in normal human subjects, *J. Lipid Res. 40*, 1194−1199.
38. Heverin, M., Bogdanovic, N., Lutjohann, D., Bayer, T., Pikuleva, I., Bretillon, L., Diczfalusy, U., Winblad, B., and Bjorkhem, I. (2004) Changes in the levels of cerebral and extracerebral sterols in the brain of patients with Alzheimer's disease, *J. Lipid Res. 45*, 186−193.
39. Mueller, E. J., Loida, P. J., and Sligar, S. G. (1995) in *Cytochrome P450: Structure, Mechanism, and Biochemistry* (Ortiz de Montellano, P. R., Ed.) pp 83−125, Plenum Publishing Corp., New York.
40. Meharenna, Y. T., Li, H., Hawkes, D. B., Pearson, A. G., De Voss, J., and Poulos, T. L. (2004) Crystal structure of P450cin in a complex with its substrate, 1,8-cineole, a close structural homologue to d-camphor, the substrate for P450cam, *Biochemistry 43*, 9487−9494.
41. Imai, M., Shimada, H., Watanabe, Y., Matsushima-Hibiya, Y., Makino, R., Koga, H., Horiuchi, T., and Ishimura, Y. (1989) Uncoupling of the cytochrome P-450cam monooxygenase reaction by a single mutation, threonine-252 to alanine or valine: possible role of the hydroxy amino acid in oxygen activation, *Proc. Natl. Acad. Sci. U.S.A. 86*, 7823−7827.
42. Hiroya, K., Ishigooka, M., Shimizu, T., and Hatano, M. (1992) Role of Glu318 and Thr319 in the catalytic function of cytochrome P450d (P4501A2): effects of mutations on the methanol hydroxylation, *FASEB J. 6*, 749−751.
43. Yeom, H., Sligar, S. G., Li, H., Poulos, T. L., and Fulco, A. J. (1995) The role of Thr268 in oxygen activation of cytochrome P450BM-3, *Biochemistry 34*, 14733−14740.
44. Vaz, A. D., Pernecky, S. J., Raner, G. M., and Coon, M. J. (1996) Peroxo-iron and oxenoid-iron species as alternative oxygenating agents in cytochrome P450-catalyzed reactions: switching by threonine-302 to alanine mutagenesis of cytochrome P450 2B4, *Proc. Natl. Acad. Sci. U.S.A. 93*, 4644−4648.
45. Domanski, T. L., Liu, J., Harlow, G. R., and Halpert, J. R. (1998) Analysis of four residues within substrate recognition site 4 of human cytochrome P450 3A4: role in steroid hydroxylase activity and alpha-naphthoflavone stimulation, *Arch. Biochem. Biophys. 350*, 223−232.
46. Okamoto, N., Imai, Y., Shoun, H., and Shiro, Y. (1998) Site-directed mutagenesis of the conserved threonine (Thr243) of the distal helix of fungal cytochrome P450nor, *Biochemistry 37*, 8839−8847.
47. Gotoh, O. (1992) Substrate recognition sites in cytochrome P450 family 2 (CYP2) proteins inferred from comparative analyses of amino acid and coding nucleotide sequences, *J. Biol. Chem. 267*, 83−90.
48. von Wachenfeldt, C., and Johnson, E. F. (1995) in *Cytochrome P450: Structure, Mechanism, and Biochemistry* (Ortiz de Montellano, P. R., Ed.) pp 183−244, Plenum Press, New York.
49. Domanski, T. L., and Halpert, J. R. (2001) Analysis of mammalian cytochrome P450 structure and function by site-directed mutagenesis, *Curr. Drug Metab. 2*, 117−137.

BI047566A